

P–O and C–O Bond Cleavages in the Thermal or Photochemical Reactions of $[\text{Fe}_2(\eta^5\text{-C}_5\text{H}_5)_2(\text{CO})_4]$ with Tetraethyl Diphosphite

Celedonio M. Alvarez, Belén Galán, M. Esther García, Víctor Riera, and Miguel A. Ruiz*

Departamento de Química Orgánica e Inorgánica/IUQOEM, Universidad de Oviedo, E-33071 Oviedo, Spain

Claudette Bois

Laboratoire de Chimie Inorganique et Matériaux Moleculaires, Université P. et M. Curie, 75252 Paris Cedex 05, France

Received March 17, 2003

The thermal and photochemical reactions of $[\text{Fe}_2\text{Cp}_2(\text{CO})_4]$ and the bidentate ligand $(\text{EtO})_2\text{POP}(\text{OEt})_2$ (tedip) proceed with different P–O or C–O bond cleavages in the diphosphite ligand. Thus, boiling toluene solutions of the above species yield the known compound $[\text{FeCp}(\text{CO})_2\{\text{P}(\text{O})(\text{OEt})_2\}]$ and the new dicarbonyl complexes $[\text{Fe}_2\text{Cp}_2\{\mu\text{-(EtO)}_2\text{POP}(\text{O})(\text{OEt})\}\{\mu\text{-P}(\text{OEt})_2\}(\text{CO})_2]$ (three isomers). The latter are slowly decarbonylated at room temperature by atmospheric oxygen to give the metal–metal-bonded complex $[\text{Fe}_2\text{Cp}_2\{\mu\text{-(EtO)}_2\text{POP}(\text{O})(\text{OEt})\}\{\mu\text{-P}(\text{OEt})_2\}(\mu\text{-CO})]$. In contrast, the photochemical reaction between the iron dimer and the diphosphite ligand gives the phosphido–phosphonate complexes $[\text{Fe}_2\text{Cp}_2\{\mu\text{-OP}(\text{OEt})_2\}\{\mu\text{-P}(\text{OEt})_2\}(\text{CO})_2]$, as a mixture of cis and trans isomers. The latter compounds experience a remarkable P–O bond reductive elimination in boiling xylenes under a CO atmosphere, whereby the diphosphite-bridged complex $[\text{Fe}_2\text{Cp}_2(\mu\text{-CO})_2(\mu\text{-tedip})]$ is formed in moderate yield. The structure of the latter was analyzed through an X-ray study. The related complexes $[\text{Fe}_2\text{Cp}_2(\mu\text{-CO})_2(\text{CO})(\kappa^1\text{-tedip})]$ and $[\{\text{Fe}_2\text{Cp}_2(\mu\text{-CO})_2(\text{CO})\}_2(\mu\text{-tedip})]$ were prepared from $[\text{Fe}_2\text{Cp}_2(\mu\text{-CO})_2(\text{CO})(\text{NCMe})]$ and the diphosphite ligand, and their role as potential precursors of the above dicarbonyl complexes was evaluated. The structures of the new complexes are analyzed on the basis of the corresponding IR and NMR (^1H , ^{31}P , ^{13}C) data, and the reaction pathways operative in these complex reactions are discussed on the basis of the available data and some cross-experiments.

Introduction

In our previous studies on the thermal and photochemical decarbonylation reactions of the binuclear compounds $[\text{M}_2\text{Cp}_2(\text{CO})_4(\mu\text{-A}_2\text{PXPAA}_2)]$ ($\text{Cp} = \eta^5\text{-C}_5\text{H}_5$; $\text{A}_2\text{-PXPAA}_2 = \text{Ph}_2\text{PCH}_2\text{PPh}_2$ (dppm), $\text{Me}_2\text{PCH}_2\text{PMe}_2$ (dmpm), $\text{M}_2 = \text{W}_2$,¹ Mo_2 ,² MoW ;³ $\text{A}_2\text{PXPAA}_2 = (\text{EtO})_2\text{POP}(\text{OEt})_2$ (tedip), $\text{M}_2 = \text{Mo}_2$, W_2 ⁴) we concluded that the unsaturated tricarbonyl intermediates initially formed in those reactions can experience three major and mutually competitive subsequent processes (Scheme 1): (a) further decarbonylation to generate a stable triple M–M bond, (b) C–H bond oxidative addition of the cyclopentadienyl ligand, or (c) P–X bond oxidative addition of the backbone of the diphosphine or diphosphite ligand.

The P–O bond cleavage was found to require lower thermal activation than the P–CH₂ cleavage, and it was also shown to be reversible. We also noticed a substantial influence of the nature of the metal (Mo or W) on the relative efficiencies of the above reaction pathways.⁴ Because of the general interest in the activation of C–H, P–C, and P–O bonds present in ligands coordinated to organometallic substrates, we decided to extend our studies to related substrates having different metal atoms. In particular, we next considered extending our studies to A_2PXPAA_2 -bridged diiron and diruthenium cyclopentadienyl complexes. In this paper we present our results on the Fe_2/tedip system, while our studies on the dppm derivatives will be reported separately.

In the first place, we noticed the lack of an appropriate starting substrate: that is, a tedip-bridged diiron-cyclopentadienyl complex. Haines and co-workers reported that the thermal or photochemical reaction between $[\text{Fe}_2\text{Cp}_2(\text{CO})_4]$ and tedip gave the phosphonate complex $[\text{FeCp}(\text{CO})_2\{\text{P}(\text{O})(\text{OEt})_2\}]$ and other noncharacterized species.⁵ It was thus clear to us that P–O bond

* To whom correspondence should be addressed. E-mail: mara@sauron.quimica.uniovi.es.

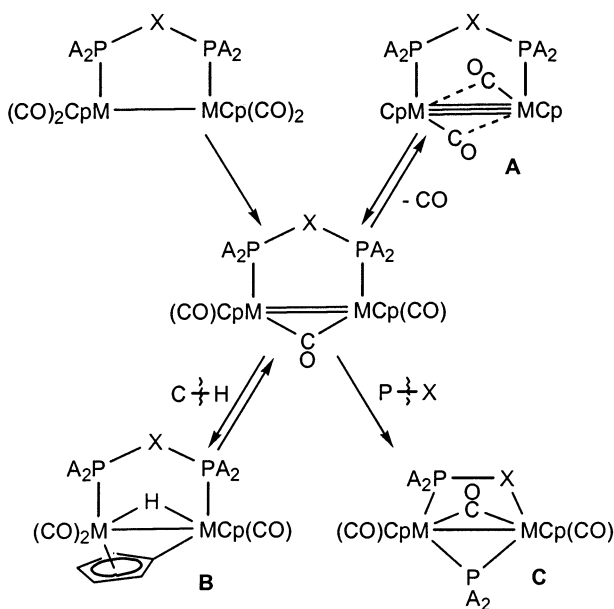
(1) (a) Alvarez, M. A.; García, M. E.; Riera, V.; Ruiz, M. A.; Falvello, L.; Bois, C. *Organometallics* **1997**, *16*, 354. (b) Alvarez, M. A.; García, M. E.; Riera, V.; Ruiz, M. A.; Falvello, L.; Bois, C.; Jeannin, Y. *J. Am. Chem. Soc.* **1993**, *115*, 3786.

(2) (a) García, G.; García, M. E.; Melón, S.; Riera, V.; Ruiz, M. A.; Villafañe, F. *Organometallics* **1997**, *16*, 626. (b) Riera, V.; Ruiz, M. A.; Villafañe, F.; Bois, C.; Jeannin, Y. *J. Organomet. Chem.* **1989**, *375*, C23.

(3) Alvarez, C.; García, M. E.; Riera, V.; Ruiz, M. A. *Organometallics* **1997**, *16*, 1378.

(4) Alvarez, M. A.; Alvarez, C.; García, M. E.; Riera, V.; Ruiz, M. A.; Bois, C. *Organometallics* **1997**, *16*, 2581.

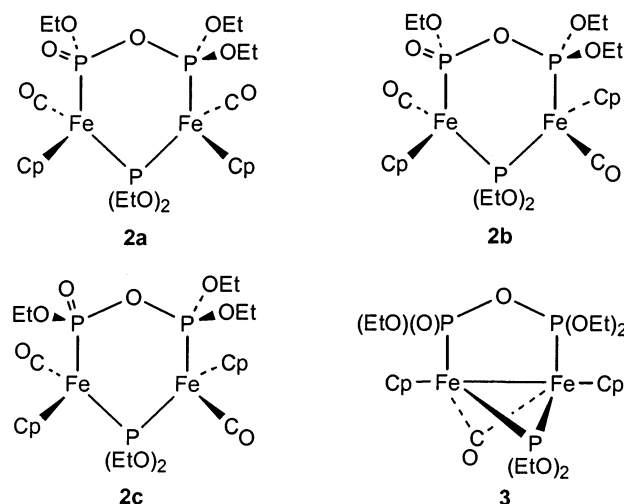
Scheme 1. The Three Different Reaction Pathways Detected during the Decarbonylation Studies of Compounds $[M_2Cp_2(CO)_4(\mu-A_2PXP_2)]$ ($M = Mo, W$; $X = CH_2, A = Ph$; $X = O, A = OEt$)¹⁻⁴



cleavages of the backbone of the tedip ligand were likely to be operating in the system, as found in our Mo and W complexes. Therefore, we decided to reinvestigate the thermal and photochemical reactions of $[Fe_2Cp_2(CO)_4]$ and tedip. Extensive studies on the thermal or photochemical^{6,7} reactions of $[Fe_2L_2(CO)_4]$ complexes ($L =$ cyclopentadienyl or related ligand) have shown that the primary species formed are the tricarbonyls $[Fe_2L_2(\mu-CO)_3]$ (isolable for $L = C_5Me_5$)⁸ and $[Fe_2L_2(\mu-\eta^1-\eta^2-CO)(CO)_2]$ (isolable for $L = C_5H_5$)⁹ and the 17-electron radicals $[FeL(CO)_2]$, resulting from homolytic cleavage of the Fe–Fe bond. None of these intermediates appear to have been recognized as being involved in the activation of coordinated ligands. We notice, however, that a C–H (cyclopentadienyl) activation occurs during the photolysis of chloroform solutions of $[Fe_2Cp_2(\mu-CO)_2(\mu-dppm)]$ to yield $[Fe_2Cp\{\eta^5-C_5H_4(CHO)\}(\mu-CO)_2(\mu-dppm)]$,^{6,10} although the relevant intermediate species have not been identified in this case.

In summary, the present study on the reactions of $[Fe_2Cp_2(CO)_4]$ (**1**) and diphosphite $(EtO)_2POP(OEt)_2$ (tedip) was initiated (a) to synthesize tedip-bridged cyclopentadienyl diiron complexes, (b) to establish the relative efficiencies of C–H (Cp) and P–O (tedip) bond cleavages at unsaturated diiron centers, and (c) to gain

Chart 1



more insight on the factors governing the ill-documented P–O cleavages of the backbone of the tedip ligand. As will be shown next, different bond cleavages in the tedip ligand are almost invariably present in all reactions studied.

Results and Discussion

Thermal Reaction of Compound **1** with tedip.

Thermal reactions between **1** and tedip were carried out at different temperatures and solvents. It was found necessary to use at least conditions of refluxing toluene in order to initiate any reaction. Best results were obtained when a 1:2 mixture of **1** and tedip was boiled in toluene for 30 min. In this way, three isomers of the formula $[Fe_2Cp_2\{\mu-(EtO)_2POP(O)(OEt)\}\{\mu-P(OEt)_2}(CO)_2]$ (**2a–c**; Chart 1) were obtained with an overall 57% yield (23%, **2a**; 22%, **2b**; 12%, **2c**). A significant amount of the known phosphonate complex $[FeCp\{P(O)(OEt)_2\}(CO)_2]$ was also formed.^{5,11} We noticed that the relative amount of the latter decreases somewhat under extreme exclusion of oxygen during the reaction. On the other hand, we also noticed that the use of a longer reaction time had no influence on the relative amount of the isomers, and no further transformations were observed either. The relative amounts of reagents had no influence on the isomer ratio, but a general decrease in all yields was observed when using equimolar mixtures of reagents, as expected. The formation of compounds **2** from **1** requires the elimination of two CO ligands, the cleavage of the metal–metal bond, and the coordination of two new three-electron-donor ligands, they being necessarily formed through important transformations in two tedip molecules which imply respectively P–O and C–O bond cleavages. The similarity in the spectroscopic data for complexes **2** (Table 1 and Experimental Section) indicates that they are structural isomers (Chart 1).

The $^{31}P\{^1H\}$ NMR spectrum for each of the isomers **2a–c** exhibits three mutually coupled signals (Table 1). The resonance at high chemical shift (ca. 350 ppm) is assigned to the phosphorus atom of a dialkoxyphosphido

(5) (a) Du Preez, A. L.; Marais, I. L.; Haines, R. J.; Pidcock, A.; Safari, M. *J. Chem. Soc., Dalton Trans.* **1981**, 1918. (b) Haines, R. J.; Du Preez, A. L. *J. Organomet. Chem.* **1971**, 28, 405.

(6) Bitterwolf, T. E. *Coord. Chem. Rev.* **2000**, 206–207, 419.

(7) (a) Wrighton, M. *Chem. Rev.* **1974**, 74, 401. (b) Hooker, R. H.; Mamound, K. A.; Rest, A. J. *J. Chem. Soc., Chem. Commun.* **1983**, 1022. (c) Zhang, S.; Brown, T. L. *J. Am. Chem. Soc.* **1992**, 114, 2723. (d) Zhang, S.; Brown, T. L. *Organometallics* **1992**, 11, 4166. (e) Zhang, S.; Brown, T. L. *J. Am. Chem. Soc.* **1993**, 115, 1779. (f) Vitale, K. K.; Lee, C. F.; Hille, R.; Gustafson, T. L.; Bursten, B. E. *J. Am. Chem. Soc.* **1995**, 117, 2286.

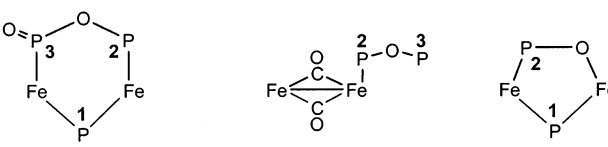
(8) Blaha, J. P.; Bursten, B. E.; Dewan, J. C.; Frankel, R. B.; Randolph, C. L.; Wilson, B. A.; Wrighton, M. A. *J. Am. Chem. Soc.* **1985**, 107, 4561.

(9) Alvarez, M. A.; Garcia, M. E.; Riera, V.; Ruiz, M. A. Unpublished results.

(10) Shade, J. E.; Pearson, W. H.; Brown, J. E.; Bitterwolf, T. E. *Organometallics* **1995**, 14, 157.

(11) The IR spectrum is in agreement with the literature report for this product.⁵ In our hands, this complex is also characterized by a broad ^{31}P NMR resonance at 104 ppm.

Table 1. IR and NMR Data for New Compounds



compd	$\nu_{\text{st}}(\text{CO})^a$	$\delta(\text{P})^b$			J_{PP}		
		P1	P2	P3	J_{12}	J_{13}	J_{23}
$[\text{Fe}_2\text{Cp}_2\{\mu\text{-(EtO)}_2\text{POP}(\text{O})(\text{OEt})\}\{\mu\text{-P}(\text{OEt})_2\}(\text{CO})_2]$ (2a)	1965 (vs), 1943 (s)	350.9	157.6	135.9	77	77	9
$[\text{Fe}_2\text{Cp}_2\{\mu\text{-(EtO)}_2\text{POP}(\text{O})(\text{OEt})\}\{\mu\text{-P}(\text{OEt})_2\}(\text{CO})_2]$ (2b)	1965 (s), 1936 (vs)	339.4	153.0	128.0	83	91	22
$[\text{Fe}_2\text{Cp}_2\{\mu\text{-(EtO)}_2\text{POP}(\text{O})(\text{OEt})\}\{\mu\text{-P}(\text{OEt})_2\}(\text{CO})_2]$ (2c)	1955 (s), 1943 (vs)	344.9	155.8	127.7	74	86	9
$[\text{Fe}_2\text{Cp}_2\{\mu\text{-(EtO)}_2\text{POP}(\text{O})(\text{OEt})\}\{\mu\text{-P}(\text{OEt})_2\}(\mu\text{-CO})]$ (3)	1763 ^c	360.4	163.2	133.0	92	92	74
<i>cis</i> - $[\text{Fe}_2\text{Cp}_2(\mu\text{-CO})_2(\text{CO})(\kappa^1\text{-tedip})]$ (cis-4)	1955 (m), 1743 (vs)		165.5 ^d	126.4 ^d			12
<i>trans</i> - $[\text{Fe}_2\text{Cp}_2(\mu\text{-CO})_2(\text{CO})(\kappa^1\text{-tedip})]$ (trans-4)	1933 (m), 1743 (vs)		168.6 ^d	126.5 ^d			
<i>trans,cis</i> - $[\{\text{Fe}_2\text{Cp}_2(\mu\text{-CO})_2(\text{CO})\}_2(\mu\text{-tedip})]$ (trans,cis-5)	1955 (m), 1933 (m), 1743 (vs)		163.0, 159.4 ^e				80
<i>cis,cis</i> - $[\{\text{Fe}_2\text{Cp}_2(\mu\text{-CO})_2(\text{CO})\}_2(\mu\text{-tedip})]$ (cis,cis-5)	1955 (m), 1743 (vs)		159.5 ^e				
<i>cis</i> - $[\text{Fe}_2\text{Cp}_2\{\mu\text{-OP}(\text{OEt})_2\}\{\mu\text{-P}(\text{OEt})_2\}(\text{CO})_2]$ (cis-6)	1972 (vs), 1962 (sh) ^c	353.8	190.4		81		
<i>trans</i> - $[\text{Fe}_2\text{Cp}_2\{\mu\text{-OP}(\text{OEt})_2\}\{\mu\text{-P}(\text{OEt})_2\}(\text{CO})_2]$ (trans-6)	1943 (sh), 1937 (vs) ^c	346.1	184.7		74		
$[\text{Fe}_2\text{Cp}_2(\mu\text{-CO})_2(\mu\text{-tedip})]$ (7)	1744 (w), 1698 (vs) ^f		179.1				

^a Recorded in toluene solution, unless otherwise stated. ν is given in cm^{-1} . ^b Recorded in C_6D_6 solution at 290 K and 121.50 MHz, unless otherwise stated. δ is given in ppm relative to external 85% aqueous H_3PO_4 ; coupling constants are given in Hertz, phosphorus atoms are labeled (P1–P3) according to the figure shown. ^c In petroleum ether. ^d In CD_2Cl_2 ; *cis*:*trans* = 9:1. ^e In toluene- d_8 solution. *cis,cis,cis,trans* = 6:1, at 253 K. Recorded in CD_2Cl_2 . ^f In CH_2Cl_2 solution. When recorded in petroleum ether, $\nu(\text{CO})$ bands appear at 1765 (vw), 1754 (vw), 1721 (vs), and 1712 (vs) cm^{-1} .

ligand, this being a shielding similar to that reported by Verkade et al. for compounds of the type $[\text{Fe}_2\text{Cp}_2\{\mu\text{-P}(\text{OR})_2\}_2(\text{CO})_2]$.¹² The second resonance appears at ca. 155 ppm, a value similar to those found for tedip-bridged dimolybdenum,⁴ dimanganese,¹³ or diiron^{5a} complexes, and is thus assigned to a phosphite-type phosphorus of a bridged group (P2 in Table 1). The third resonance, however, exhibits a significantly lower chemical shift (ca. 130 ppm), indicative of a relevant transformation in the corresponding phosphorus atom (P3 in Table 1). In fact, there are different pieces of evidence that conclusively establish the loss of an ethyl group from tedip to generate the three-electron-donor bridging ligand $(\text{EtO})_2\text{POP}(\text{O})(\text{OEt})$. (a) The ^1H NMR spectra of compounds **2a–c** exhibit in each case five inequivalent resonances for the methyl groups. (b) The solid-state IR spectrum of **2b** exhibits a band at ca. 1155 cm^{-1} , which can be assigned to the P–O stretch of a P=O bond, reported to appear in the range 1200–1100 cm^{-1} .^{5b,14} (c) The ^{13}C NMR spectrum of either **2a** or **2b**, recorded with selective decoupling of the P3 resonance, revealed decoupling in just one of the five inequivalent OEt resonances. In agreement with this formulation, the mass spectra of **2a,b** displayed in both cases the corresponding molecular ions at m/z 648. The P–P couplings for compounds **2** do not change much from one isomer to other (Table 1), thus suggesting that the relative arrangement of both phosphorus ligands is the same in all these isomers. Two-bond coupling between the phosphido atom (P1) and the phosphite (P2) or

phosphonate (P3) groups of the bidentate ligand are kept around 80 Hz, in agreement with the PMP angles expected (ca. 120°) for an almost flat $\text{M}_2\text{P}_3\text{O}$ ring. In contrast, the coupling inside the bidentate ligand exhibits a considerably lower value ($J_{23} = 9\text{--}22$ Hz), an effect which can be attributed to the presence of an oxygen atom (rather than a metal) connecting the phosphorus nuclei.¹⁵

The main difference among isomers **2a–c** stems from their distinct arrangement of the carbonyl ligands, in all cases being one terminal CO group bonded to each iron center, as deduced from the ^{13}C NMR and IR spectra. The latter are specially informative, as they show the pattern characteristic of $\text{M}_2(\text{CO})_2$ oscillators having a cisoid (**2a**) or transoid (**2b,c**) geometry.¹⁶ On the basis of the higher steric demands of the Cp groups (relative to the CO ligands) we propose for isomer **2a** to adopt just one out of the two possible *cis* isomers, that one having the Cp group close to the P=O moiety (Chart 1). For the same reason, in the case of the *trans* isomers we propose for the more abundant isomer (**2b**) the same local environment.

We finally note that the IR spectra of compounds **2**, when recorded in petroleum ether, exhibit an additional shoulder close to one of the two main bands. This can be attributed to the presence in solution of rapidly interconverting isomers differing in the orientation of the OEt groups, as previously found for the tedip-bridged complexes $[\text{Fe}_2(\mu\text{-CO})(\text{CO})_{8-2x}(\mu\text{-tedip})_x]$ ($x = 1, 2$).^{5a}

Oxygen-Induced Decarbonylation of Compounds

2. When solutions of **2a,b** in petroleum ether or THF are stirred at room temperature in contact with air, black-brown suspensions or solutions are slowly formed. These were shown to contain $[\text{Fe}_2\text{Cp}_2\{\mu\text{-(EtO)}_2\text{POP}(\text{O})(\text{OEt})\}\{\mu\text{-P}(\text{OEt})_2\}(\mu\text{-CO})]$ (**3**) as the major species.

(15) Jameson, C. J. In *Phosphorus-31 NMR Spectroscopy in Stereochemical Analysis*; Verkade, J. G., Quin, L. D., Eds. VCH: Deerfield Beach, FL, 1987; Chapter 6.

(16) Braterman, P. S. *Metal Carbonyl Spectra*; Academic Press: London, 1975; Chapter 3.

(12) Spencer, J. T.; Spencer, J. A.; Jacobson, R. A.; Verkade, J. G. *New J. Chem.* **1989**, 13, 275.

(13) (a) Gimeno, J.; Riera, V.; Ruiz, M. A.; Manotti-Lanfredi, A. M.; Tiripicchio, A. *J. Organomet. Chem.* **1984**, 268, C13. (b) Riera, V.; Ruiz, M. A.; Tiripicchio, A.; Tiripicchio-Camellini, M. *J. Chem. Soc., Chem. Commun.* **1985**, 1505. (c) Riera, V.; Ruiz, M. A.; Tiripicchio, A.; Tiripicchio-Camellini, M. *J. Chem. Soc., Dalton Trans.* **1987**, 1551. (d) Carreño, R.; Riera, V.; Ruiz, M. A.; Bois, C.; Jeannin, Y. *Organometallics* **1993**, 12, 1946.

(14) (a) Bellamy, L. J. *The Infrared Spectra of Complex Molecules*; Wiley: New York, 1975; Chapter 18. (b) Wong, E. H.; Ravenelle, R. M.; Gabe, E. J.; Lee, F. L.; Prasaad, L. *J. Organomet. Chem.* **1982**, 233, 321.

Compound **3** results from decarbonylation of isomers **2a,b** with a change in the coordination mode of the remaining CO ligand (from terminal to bridging mode) and the formation of a new Fe–Fe bond. This reaction can be then considered as resulting from oxidation of a CO ligand by atmospheric oxygen to form CO₂, much in the same way as the well-known decarbonylation reactions induced by Me₃NO and related amine oxides.¹⁷ Usually, however, CO oxidation by oxygen is accompanied by coordination of oxygen atoms to the metal, as either terminal or bridging ligands.^{18,19}

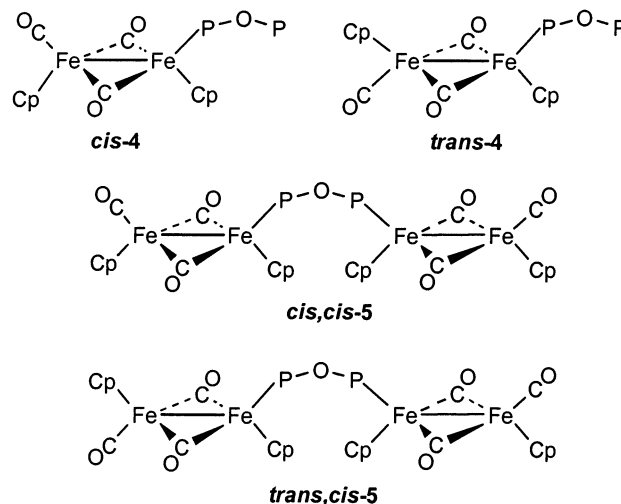
The signals observed in the ³¹P{¹H} NMR spectrum of compound **3** (Table 1) display chemical shifts and P–P couplings similar to those present in the spectra of **2**, indicating that the phosphorus ligands keep the same coordination mode and similar spatial arrangement. The same can be deduced from the ¹H NMR spectrum, this revealing the presence of two inequivalent Cp ligands and five different ethoxy groups. The most significant change in the NMR data for **3** is the strong increase of the coupling between the phosphite- and phosphonate-type phosphorus nuclei (*J*₁₃ = 74 Hz). This can be attributed to the presence of the new metal–metal bond, which allows a new (PMMP) three-bond contribution to the coupling, now added to the small two-bond contribution (POP) already present in isomers **2**.

The IR spectrum of **3** in the solid state exhibits an absorption at 1172 cm⁻¹, which can be assigned to the P–O stretch of a P=O bond, showing that this structural feature remains intact in the molecule. The IR spectrum in solution displays just one band in the CO stretching region. Its low frequency (1763 cm⁻¹) is clearly indicative of a bridging coordination mode for this ligand.¹⁶

Synthesis and Structure of Tricarbonyl Derivatives with tedip Ligands. As we have just discussed, the thermal reaction between **1** and tedip does not lead to the formation of any tedip-bridged diiron derivative. This is in contrast with the behavior of the dppm ligand under similar conditions, reported to give the bridged derivative [Fe₂Cp₂(μ-CO)₂(μ-dppm)] in high yield.²⁰ To prepare a similar tedip-bridged dicarbonyl compound, we then considered carrying out substitution reactions on suitable labile precursors of the type [Fe₂Cp₂(CO)₃(L)], such as the acetonitrile adduct [Fe₂Cp₂(CO)₃(NCMe)].²¹ It is well-known that the acetonitrile ligand is weakly coordinated to the iron atom in this compound and that it can be substituted very easily by two-electron-donor ligands. As expected, the tricarbonyl compound [Fe₂Cp₂(CO)₃(NCMe)] reacts rapidly with tedip in toluene even at 0 °C to give either the dinuclear [Fe₂Cp₂(μ-CO)₂(CO)(κ¹-tedip)] (**4**) or the tetranuclear complex [{Fe₂Cp₂(μ-CO)₂(CO)}₂(μ-tedip)] (**5**) (Chart 2), depending on the stoichiometry used.

Compound **4** is a rare example of a metal complex having a tedip ligand coordinated through a single phosphorus atom. This is clearly shown in the ³¹P{¹H}

Chart 2



NMR spectrum, which exhibits two weakly coupled doublets. The signal at 165.5 ppm (Table 1) has the chemical shift expected for tedip-bridged complexes,^{4,5a,13} while the signal at 126.4 ppm has a chemical shift very close to that for the free tedip ligand (128.4 ppm in C₆D₆). Therefore, it can be safely assigned to the uncoordinated phosphorus atom of a κ¹-tedip group. In addition to these signals, the ³¹P spectra of **4** always exhibit a weaker pair of doublets, which we assign to a minor isomer of compound **4**. This can be confirmed through the IR spectrum, where, in addition to the strong band observed in the bridging C–O frequencies, there are two bands in the terminal C–O region. This has been observed in the isostructural complexes [Fe₂Cp₂(μ-CO)₂(CO){P(OR)₃}]²² where cis and trans isomers are present and can be distinguished through the frequency of the terminal C–O stretch, which is higher for the cis isomer. We then conclude that **cis-4** is the major isomer present in the solutions of this compound.

Compound **4** is air sensitive (as is the free ligand itself), probably due to the presence of a tedip ligand coordinated through just one phosphorus atom. When the compound is heated in toluene at 80 °C for 1 h, complete decomposition occurs to yield [Fe₂Cp₂(CO)₄] and [FeCp{P(O)(OEt)₂}(CO)₂]. No other species could be detected by IR or ³¹P NMR monitoring of this reaction.

Complex **5** exhibits stretching C–O bands identical with those of compound **4**. The presence of terminal and equivalent bridging CO ligands has been also confirmed through the ¹³C{¹H} NMR spectrum, which also denotes the presence of double number of bridging than terminal CO ligands. The ¹H NMR spectrum of complex **5** exhibits two signals corresponding to the Cp ligands but a single triplet for the OEt groups of the ligand (relative intensities 10:10:12). The implied equivalence of both phosphorus atoms of the tedip ligand is corroborated by the ³¹P{¹H} NMR spectrum at room temperature, which exhibits a singlet resonance at 158.9 ppm, as expected. All this supports an structure built from two *cis*-[Fe₂Cp₂(μ-CO)₂(CO)] moieties bridged by the diphosphite ligand (**cis,cis-5**, Chart 2). A closer inspection of the ³¹P spectrum at room temperature reveals the presence of a weaker, broad resonance at 162.0 ppm.

(17) Cotton, F. A.; Wilkinson, G. *Advanced Inorganic Chemistry*, 5th ed.; Wiley: New York, 1988; Chapter 22.

(18) Riera, V.; Ruiz, M. A.; Villafañe, F.; Bois, C.; Jeannin, Y. *Organometallics* **1993**, *12*, 124.

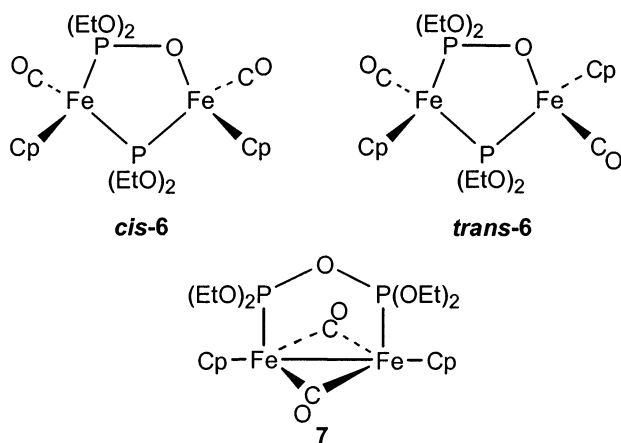
(19) Bottomley, F.; Sutin, L. *Adv. Organomet. Chem.* **1988**, *28*, 339.

(20) Haines, R. J.; Du Preez, A. L. *J. Organomet. Chem.* **1970**, *21*, 181.

(21) Labinger, J. A.; Madhavan, S. *J. Organomet. Chem.*, **1977**, *134*, 381.

(22) Haines, R. J.; Du Preez, A. L. *Inorg. Chem.* **1969**, *8*, 1459.

Chart 3



When the $^{31}P\{^1H\}$ NMR spectrum is recorded at 253 K, this broad resonance splits into two doublets at 163.0 and 159.4 ppm with a coupling constant of 80 Hz. By comparing these values with that of the major isomer **cis-cis-5** and taking into account the relative ^{31}P shifts in the isomers present in **4** ($\delta_{trans} - \delta_{cis} = 3$ ppm), we propose the minor isomer to be **trans-cis-5** (Chart 2). This is in agreement with the presence of a shoulder at 1933 cm^{-1} in the IR spectrum of toluene solutions of **5** (Table 1) and with the lack of equivalence of the corresponding four Cp ligands (only three of the corresponding resonances located in the 1H NMR spectrum at 253 K).

Photochemical Reactions of Compound 1 with Tedip. As stated above, the photochemical reaction between **1** and tedip was studied by Haines in 1981,^{5a} but only the mononuclear complex $[FeCp\{P(O)(OEt)_2\}(CO)_2]$ could be isolated and identified from the corresponding reaction mixtures. We have now reinvestigated this reaction, and we have found results quite different from either our thermal reaction or the previous photochemical results.

Photolysis of stoichiometric amounts of **1** and tedip leads to a mixture of the dicarbonyl compounds *cis*- and *trans*- $[Fe_2Cp_2\{\mu-OP(OEt)_2\}\{\mu-P(OEt)_2\}(CO)_2]$ (**cis-6** and **trans-6**, Chart 3) in good yield (ca. 1:1 ratio). Best results are obtained using low reaction temperatures ($-15\text{ }^\circ\text{C}$) and toluene as a solvent. We have also found that the reaction time has no significant influence on the ratio of isomers, although prolonged photolysis leads to a decrease in the overall yield. The formation of these two isomers involve the elimination of two molecules of CO, cleavage of the Fe–Fe bond, and the activation of one of the P–O bonds of the backbone of the tedip ligand, to give two new bridging three-electron-donor ligands (the diethoxyphosphido and diethylphosphonate bridges).

The structure of isomers **6** has been proposed on the basis of the corresponding spectroscopic data and comparison with data for the related complexes $[M_2Cp_2\{\mu-OP(OEt)_2\}\{\mu-P(OEt)_2\}(CO)_2]$ ($M = Mo, W$)⁴ and $[Fe_2Cp_2\{\mu-N(Ph)P(OPh)_2\}\{\mu-P(OPh)_2\}(CO)_2]$.²³ The 1H and $^{31}P\{^1H\}$ NMR spectra of compounds **6** are very similar, as expected for *cis* and *trans* isomers (Table 1 and Experimental Section). Each of the isomers displays two

resonances at ca. 350 and 190 ppm. The less shielded resonances appear in the usual region for the alkoxyphosphido bridging ligands (400–250 ppm),^{4,12} while the other resonances appear in the expected range for diethylphosphonate bridging Mo, W, or Mn binuclear complexes (200–150 ppm).^{4,24} The 1H and $^{13}C\{^1H\}$ NMR spectra for both isomers are consistent with the proposed structure, which implies the presence of two signals for the Cp ligands and four different sets assigned to the inequivalent ethoxy groups. The dicarbonyl nature of both isomers is confirmed by their $^{13}C\{^1H\}$ NMR and IR spectra. As expected, the ^{13}C carbonyl resonances exhibit coupling to one or two phosphorus nuclei, depending on the iron atom to which these CO ligands are coordinated. The identification of the *cis* and *trans* isomers is derived from the IR spectra recorded in petroleum ether, which then exhibit two sharp bands in the region of the terminal C–O stretches. The relative intensity of these bands, weak and strong for one isomer and strong and weak (in order of decreasing frequency) for the other one, allow us to identify them as *trans* and *cis* isomers, respectively.¹⁶

Synthesis and Structure of $[Fe_2Cp_2(\mu-CO)_2(\mu-tedip)]$ (7**).** When the photochemical reaction of **1** and tedip is carried out at $15\text{ }^\circ\text{C}$, a mixture of isomers **6** and ca. 5% of the tedip-bridged $[Fe_2Cp_2(\mu-CO)_2(\mu-tedip)]$ (**7**, Chart 3) is obtained. Unfortunately, we have not been able to improve the yield of complex **7** by changing the experimental conditions of the photolysis. We also note that photolysis of toluene solutions of the tricarbonyl **4**, a complex with the right structure to yield **7** after CO ejection, apparently gives **7** cleanly, as deduced from the IR and ^{31}P spectra of the reaction mixture, but the yield after chromatography of the reaction mixture is very low.

The best synthetic route we have found for **7** is based on the high-temperature transformation **6/7** under a CO atmosphere. This requires the reductive elimination of a P–O bond between the diethoxyphosphido group and the diethylphosphonate ligand to regenerate the tedip molecule, a process previously observed only at Mo_2 centers.⁴ In this way, complex **7** can be isolated in an overall yield of 15% (based on $[Fe_2Cp_2(CO)_4]$), which means that the P–O bond reductive elimination step has an efficiency of ca. 50%. Once formed, the tedip-bridged **7** cannot be converted back into the phosphido precursors **6** either in refluxing xylenes or under visible–UV irradiation.

The structure of **7** has been solved through an X-ray study and is depicted in Figure 1, while Table 2 lists the most relevant bond distances and angles. The molecule displays two iron cyclopentadienyl fragments bridged by a tedip and two carbonyl ligands. The Fe_2P_2O ring defined by the diphosphite and iron atoms is almost flat, and the bridging carbonyls lie almost in a plane perpendicular to it (see projection in Figure 1). The intermetallic separation ($Fe1-Fe2 = 2.512(2)\text{ \AA}$) is very similar to the values found (ca. 2.52 \AA) for the diphosphine-bridged $[Fe_2CpCp'(\mu-CO)_2(\mu-Ph_2PCH_2CH_2PPh_2)]$ ($Cp' = C_5H_5, C_5H_4CHO$)¹⁰ and shorter than the tedip-

(23) Balakrishna, M. S.; Krishnamurthy, S. S. *Indian J. Chem.* **1991**, *30A*, 536.

(24) (a) Liu, X. Y.; Riera, V.; Ruiz, M. A.; Lanfranchi, M.; Tiripicchio, A.; Tiripicchio-Camellini, M. *Organometallics* **1994**, *13*, 1940. (b) Liu, X. Y.; Riera, V.; Ruiz, M. A.; Tiripicchio, A.; Tiripicchio-Camellini, M. *Organometallics* **1996**, *15*, 974.

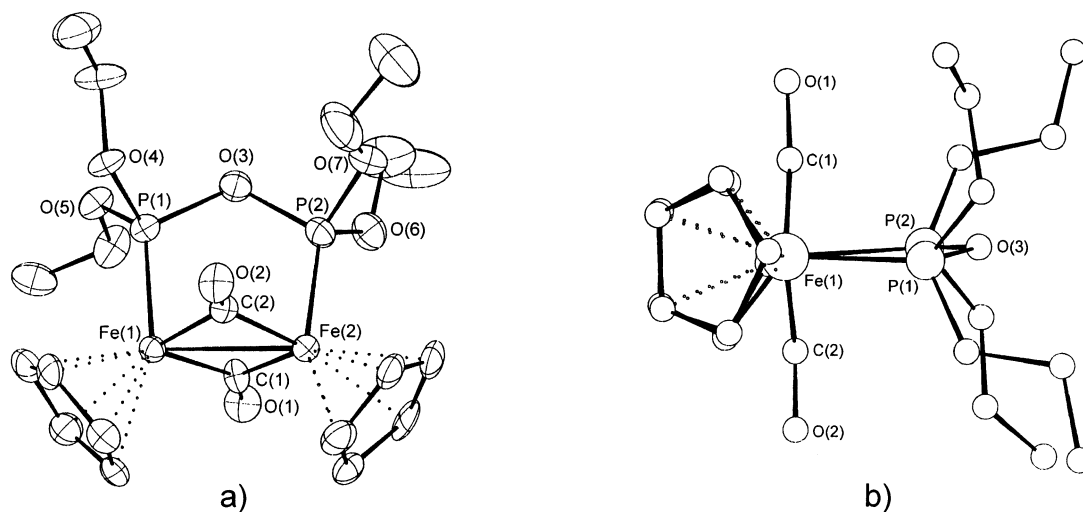


Figure 1. (a) CAMERON diagram of the molecular structure of compound **7**. Ellipsoids represent 30% probability. (b) View of the molecule along the Fe–Fe direction.

Table 2. Selected Bond Distances (Å) and Angles (deg) for Compound 7

<i>d</i> (Å)		θ (deg)	
Fe(1)–Fe(2)	2.512(2)	Fe(2)–Fe(1)–P(1)	94.6(1)
Fe(1)–P(1)	2.111(4)	Fe(1)–Fe(2)–P(2)	94.7(1)
Fe(2)–P(2)	2.101(4)	Fe(1)–C(1)–Fe(2)	82.3(5)
Fe(1)–C(1)	1.91(1)	Fe(1)–C(2)–Fe(2)	82.5(5)
Fe(2)–C(1)	1.90(1)	Fe(1)–C(1)–O(1)	138.7(10)
Fe(1)–C(2)	1.92(1)	Fe(2)–C(1)–O(1)	138.6(10)
Fe(2)–C(2)	1.90(1)	Fe(1)–C(2)–O(2)	136.7(10)
P(1)–O(3)	1.659(8)	Fe(2)–C(2)–O(2)	140.1(10)
P(2)–O(3)	1.631(9)	P(1)–O(3)–P(2)	120.9(5)
P(1)–O(4)	1.587(9)	Fe(1)–P(1)–O(3)	114.0(3)
P(1)–O(5)	1.605(9)	Fe(2)–P(2)–O(3)	115.1(3)
P(2)–O(6)	1.59(1)	O(4)–P(1)–O(5)	98.9(4)
P(2)–O(7)	1.59(1)	O(6)–P(2)–O(7)	98.2(6)
O(1)–C(1)	1.18(1)	C(1)–Fe(2)–P(2)	87.9(4)
O(2)–C(2)	1.17(1)	C(1)–Fe(1)–P(1)	92.0(4)
		C(2)–Fe(2)–P(2)	91.4(4)
		C(2)–Fe(1)–P(1)	87.4(4)

bridged iron(0) complex $[\text{Fe}_2(\mu\text{-CO})(\text{CO})_4(\mu\text{-tedip})_2]$ (2.666(2) Å),²⁵ as expected.

Spectroscopic data in solution for **7** are consistent with the highly symmetric solid-state structure. This is reflected in the chemical equivalence of both phosphorus atoms and of cyclopentadienyl and ethoxy H and C nuclei (Table 1 and Experimental Section). The IR spectrum of **7** in most solvents exhibits, around 1700 cm^{-1} , a very weak band and a strong band in order of decreasing frequency, in agreement with the presence of two bridging carbonyls defining almost a 180° relative angle.¹⁶ When recorded in petroleum ether, however, both bands appear split. As the NMR spectra of **7** in toluene-*d*₈ remained unchanged down of –90 °C, we rather attribute this splitting of the $\nu(\text{CO})$ bands to the presence of two very similar conformers, rapidly interconverting on the NMR time scale. In fact, when recording the IR spectrum of a petroleum ether solution freshly prepared from crystals of **7**, we observe first the predominance of those bands at 1765 (vw) and 1721 (vs) cm^{-1} , but then bands at 1754 (vw) and 1712 (vs) cm^{-1} progressively grow so as to reach an intensity comparable to that of the former bands after 1 h. No further changes occur in the spectrum. All this suggests that

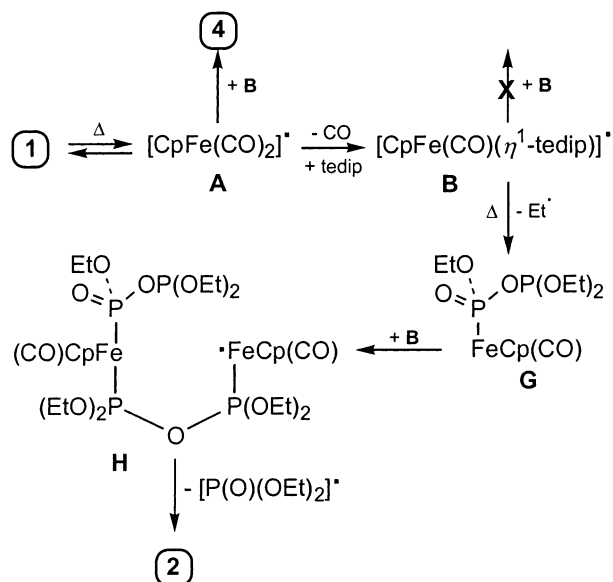
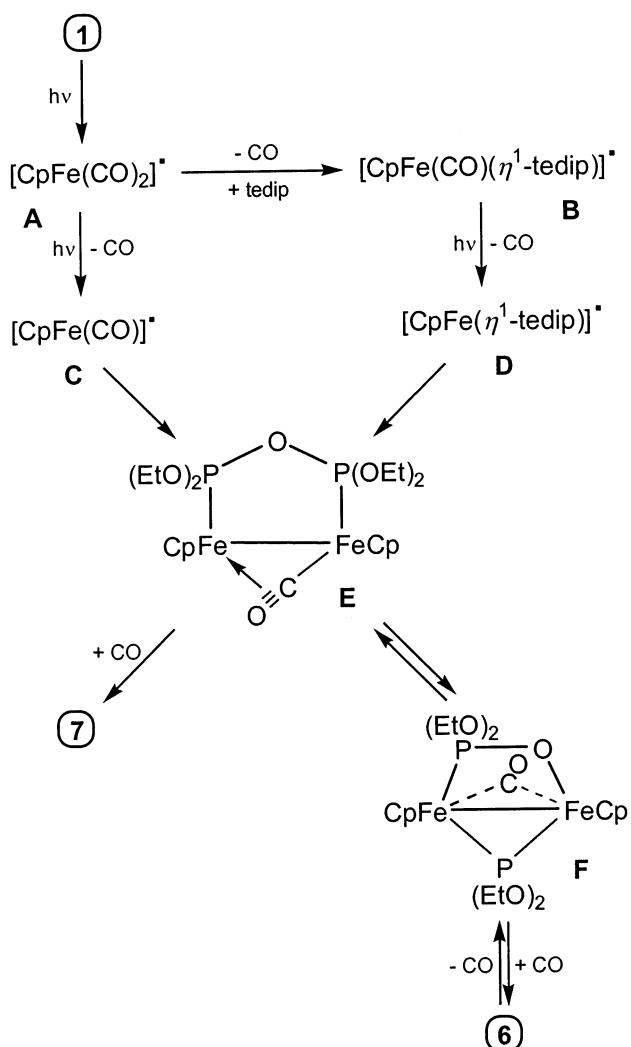
the two first-mentioned bands correspond to the molecule present in the crystal, while the other two bands would arise from a slight structural modification of the former. We note again that complexes $[\text{Fe}_2(\mu\text{-CO})(\text{CO})_{8-2x}(\mu\text{-tedip})_x]$ ($x = 1, 2$)²⁵ also exhibit splitting of the bridging CO bands, which has been explained in terms of more than one conformer in solution resulting from different relative orientations of ethoxy groups in the tedip ligand.

Reaction Pathways of tedip at Diiron Centers.

As we have just discussed, the diphosphite ligand tedip reacts with $[\text{Fe}_2\text{Cp}_2(\text{CO})_4]$ to give mainly products derived of the cleavage of either C–O (compounds **2**) or P–O bonds (compounds **2** and **6**) of the ligand. The simple substitution product **7** is obtained only in low yields under photochemical conditions and room temperature. All those products require several elementary steps to be formed; thus, the detailed reaction pathways in operation must be necessarily complex and cannot be inferred from a synthetic work. Despite this, by taking into account all our data and the general knowledge available on the decarbonylation reactions of **1**, we can draw a rational picture of the main reaction pathways likely to be operative in the system under study (Schemes 2 and 3).

As stated in the Introduction, substitution reactions on compound **1** can occur through initial CO dissociation or homolytic cleavage of the Fe–Fe bond. In the first case, this would be expectedly followed by addition of the ligand to give the tricarbonyl complex **4**. However, we have shown through separate experiments that neither thermal nor photochemical treatment of **4** give significant amounts of either **2** or **6**. From this we conclude that initial CO dissociation from **1** is not a significant pathway in the reactions under study. We rather trust that both the thermal and the photochemical reactions between **1** and tedip are initiated by the homolytic cleavage of the Fe–Fe bond to give the $[\text{FeCp}(\text{CO})_2]$ radical **A**,^{6,7} which is well-known to experience easy CO substitution by ligands. In our case, **A** would thus easily give the 17-electron tedip derivative $[\text{FeCp}(\text{CO})(\kappa^1\text{-tedip})]$ (**B**).^{7c} At this point, three radical recombinations can occur: **A–A**, **A–B** or **B–B** (Scheme 2). The first one affords the starting complex **1**, which

(25) Cotton, F. A.; Haines, R. J.; Hanson, B. E.; Sekutowski, J. C. *Inorg. Chem.* **1978**, *17*, 2010.

Scheme 2. Proposed Reaction Pathways in the Thermal Reaction of 1 and tedip**Scheme 3. Proposed Reaction Pathways in the Photochemical Reaction of 1 and tedip**

obviously must be in equilibrium with radical **A** under photolytic conditions. Reaction **A** + **B** would give compound **4**, but this cannot account for the formation

of complexes **2** and **6**, as stated above. The dimerization process **B** + **B** could happen as well, but this is expected to be slow, as shown for other phosphine-substituted radicals of the type $[\text{FeCp}(\text{CO})(\text{L})]^\bullet$. As a result, further evolution of the radicals **A** and **B**, different from simple recombination, should be involved in order to explain our experimental results.

Under thermal conditions, we propose that elimination of an ethyl radical occurs from **B**, as has been observed before in the reaction of the rhodium dimer $[\text{Rh}_2\text{L}_4]_2$ ($\text{L}_4 = \text{porphyrin ligand}$) with trimethyl phosphite.²⁶ This would lead to the formation of the 16-electron intermediate **G**, which rapidly would react with any 2-electron ligand available, for instance the uncoordinated phosphorus atom of radical **B**, to give the dinuclear radical **H**. This complex could evolve by extrusion of a $\text{P}(\text{O})(\text{OEt})_2$ radical to finally give complex **2**. We note that the phosphonate radical $[\text{P}(\text{O})(\text{OEt})_2]^\bullet$ has been proposed as a precursor in several syntheses of phosphonate complexes.²⁷ Reaction of the latter radical with intermediate **A** also explains the appearance of significant amounts of the complex $[\text{FeCp}\{\text{P}(\text{O})(\text{OEt})_2\}(\text{CO})_2]$ in our thermal reactions.

Under photochemical conditions, it is proposed that either of the radicals **A** and **B** could experience further decarbonylation to give 15-electron radicals.^{7c} In our case, this would lead to radicals **C** and **D**, the combination of which would give the monocarbonyl intermediate **E**, isoelectronic with the compound $[\text{Fe}_2\text{Cp}_2(\mu\text{-}\eta^1\text{-}\eta^2\text{-CO})(\text{CO})_2]^{6b,9}$ and also having probably a $\mu\text{-}\eta^1\text{-}\eta^2$ bridging CO ligand. This intermediate could lead to the formation of complex **7** after carbonylation or to complexes **6** by intramolecular oxidative addition of a P–O bond of the tedip ligand, via intermediate **F**, and further carbonylation. The transformations **7/E/F/6** are similar to those previously postulated to explain the thermal isomerization between $[\text{Mo}_2\text{Cp}_2\{\mu\text{-}(\text{EtO})_2\text{POP}(\text{OEt})_2\}(\text{CO})_4]$ and $[\text{Mo}_2\text{Cp}_2\{\mu\text{-OP}(\text{OEt})_2\}\{\mu\text{-P}(\text{OEt})_2\}(\text{CO})_4]$.⁴ Our experimental observations indicate that the transformation **E/F** would be reversible, with a significant influence of temperature on the equilibrium ratio. At high temperatures the tedip-bridged **E** would dominate, while phosphonate **F** would prevail at low temperature. This hypothesis explains the photochemical production of just complex **6** at -30°C and the appearance of moderate amounts of **7** in the room-temperature photolytic experiments. On the other hand, this hypothesis gives a rationale for the high-temperature transformation of **6** into **7** and the observation that the yield increases in the presence of CO.

Conclusion

The reactions between $[\text{Fe}_2\text{Cp}_2(\text{CO})_4]$ and the diphosphite ligand $(\text{EtO})_2\text{POP}(\text{OEt})_2$ seem to proceed mainly through the radical intermediates $[\text{FeCp}(\text{CO})_2]^\bullet$ and $[\text{FeCp}(\text{CO})(\eta^1\text{-tedip})]^\bullet$, which invariably experience additional C–O (ethoxy) or P–O (backbone) bond cleavages of the phosphorus ligand, but no activation of the C–H bonds in the cyclopentadienyl ligand. Under

(26) Wayland, B. B.; Woods, B. A. *J. Chem. Soc., Chem. Commun.* **1981**, 475.

(27) Goh, L. Y.; D'Aniello, M. J., Jr.; Slater, S.; Muetterties, E. L.; Tavanaiepour, I.; Chang, M. I.; Fredrich, M. F.; Day, V. W. *Inorg. Chem.* **1979**, *18*, 192.

thermal activation, both the above cleavages occur, to generate phosphite–phosphonate (μ -(EtO)₂POP(O)-(OEt)) and phosphonate (μ -OP(OEt)₂) bridging groups. Under photochemical conditions, backbone P–O bond oxidative addition of the tedip ligand dominates, to give phosphonate and alkoxyphosphido [μ -P(OEt)₂] bridging groups, even at –25 °C. This last transformation is reversible, and PO bond reductive elimination to regenerate the tedip ligand can be forced in refluxing xylenes.

Experimental Section

General Comments. All manipulations and reactions were carried out using standard Schlenk techniques under an atmosphere of dry, oxygen-free nitrogen. Solvents were purified according to standard literature procedures²⁸ and distilled under nitrogen prior to use. Petroleum ether refers to the fraction distilling in the range 60–65 °C. The compound [Fe₂Cp₂(CO)₃(NCMe)] was prepared as described previously.²¹ The compounds [Fe₂Cp₂(CO)₄] and tedip were obtained from the usual commercial suppliers and used without further purification. Photochemical experiments were performed using jacketed Pyrex or quartz Schlenk tubes, refrigerated by a closed 2-propanol circuit kept at the desired temperature with a cryostat or by tap water. A 400 W mercury lamp (Applied Photophysics), placed ca. 1 cm away from the Schlenk tube, was used for these experiments. Low-temperature chromatographic separations were carried out analogously using jacketed columns. Commercial aluminum oxide (Aldrich, activity I, 150 mesh) was degassed under vacuum prior to use. The latter was mixed afterward under nitrogen with the appropriate amount of water to reach the activity desired. Filtrations were carried out using diatomaceous earth. NMR spectra were recorded at 400.13 (¹H), 163.01 (³¹P{¹H}), or 100.62 MHz (¹³C-{¹H} and ¹³C{¹H, ³¹P}), at room temperature unless otherwise stated. Chemical shifts (δ) are given in ppm, relative to internal TMS (¹H, ¹³C) or external 85% H₃PO₄ aqueous solution (³¹P), with positive values for frequencies higher than that of the reference. Coupling constants (J) are given in hertz. ¹³C-{¹H} NMR spectra were routinely recorded on solutions containing a small amount of tris(acetylacetonato)chromium(III) as a relaxation reagent.

Preparation of Isomers [Fe₂Cp₂{ μ -(EtO)₂POP(O)(OEt)}- μ -P(OEt)₂(CO)₂] (2). A toluene solution (15 mL) of compound **1** (0.300 g, 0.84 mmol) and tedip (0.26 mL, 1.06 mmol) was refluxed for 30 min to give a yellow-orange solution. This solution was concentrated under vacuum and chromatographed at –15 °C on an alumina column (activity 3.5, 30 \times 2.5 cm) prepared in petroleum ether. Elution with THF/petroleum ether (1:5) gave a yellow fraction containing a mixture of compounds that were not identified. Elution with THF/petroleum ether (1:2) gave two yellow fractions containing isomers **2a**, **b**, respectively. Elution with THF/petroleum ether (3:1) gave a third yellow fraction containing isomer **2c**. Finally, elution with pure THF gave a yellow-orange fraction containing the compound [FeCp₂{P(OEt)₂}(CO)₂]. Removal of solvents under vacuum from the different fractions gave respectively compounds **2a** (0.100 g, 23%), **2b** (0.094 g, 22%), and **2c** (0.054 g, 12%) as yellow oily solids. The latter can be converted into microcrystalline powders after recrystallization from petroleum ether solutions at –20 °C. Data for **2a** are as follows. Anal. Calcd for C₂₂H₃₅O₉P₃Fe₂: C, 40.77; H, 5.44. Found: C, 41.02; H, 5.42. ¹H NMR (200.13 MHz, C₆D₆): δ 4.73, 4.72 (2 \times s, 2 \times 5H, Cp), 4.40–3.60 (m, 10H, CH₂), 1.38, 1.28, 1.19, 1.12, 1.08 (5 \times t, $J_{\text{HH}} = 7$, 5 \times 3H, Me). ³¹P{¹H} NMR (80.01 MHz, C₆D₆): δ 350.9 (t, $J_{\text{PP}} = 77$, μ -P, P1), 157.7 (dd, $J_{\text{PP}} = 77$, 9, [P(OEt)₂], P2), 135.9 (dd, $J_{\text{PP}} = 77$, 9, [P(O)(OEt)], P3). ¹³C-

{¹H} NMR (100.63 MHz, C₆D₆, assignment of PC couplings from selectively decoupled spectra): δ 218.8 (dd, $J_{\text{CP3}} = 52$, $J_{\text{CP1}} = 23$, CO), 217.5 (dd, $J_{\text{CP2}} = 41$, $J_{\text{CP1}} = 20$, CO), 85.6, 84.1 (2 \times s, Cp), 61.6 (d, $J_{\text{CP2}} = 8$, CH₂), 61.4 (d, $J_{\text{CP1}} = 7$, CH₂), 61.3 (d, $J_{\text{CP2}} = 9$, CH₂), 61.1 (d, $J_{\text{CP1}} = 9$, CH₂), 58.2 (d, $J_{\text{CP3}} = 9$, CH₂), 17.4 (d, $J_{\text{CP3}} = 5$, Me), 16.3 (d, $J_{\text{CP2}} = 6$, Me), 16.05, 16.00 (2 \times d, $J_{\text{CP1}} = 7$, $J_{\text{CP2}} = 7$, 2 \times Me), 15.4 (d, $J_{\text{CP1}} = 5$, Me). FAB-MS: m/z (%) 648(15) [M⁺], 620(85) [M⁺ – CO], 603(100) [M⁺ – OEt], 528(75) [M⁺ – CO – P(O)(OEt)]. Data for **2b** are as follows. Anal. Calcd for C₂₂H₃₅O₉P₃Fe₂: C, 40.77; H, 5.44. Found: C, 40.95; H, 5.51. ¹H NMR (200.13 MHz, C₆D₆): δ 4.66, 4.62 (2 \times s, 2 \times 5H, Cp), 4.50–3.60 (m, 10H, CH₂), 1.39, 1.31, 1.28, 1.13, 1.09 (5 \times t, $J_{\text{HH}} = 7$, 5 \times 3H, Me). ³¹P-{¹H} NMR (80.01 MHz, C₆D₆): δ 339.5 (dd, $J_{\text{PP}} = 91$, 83, μ -P, P1), 153.1 (dd, $J_{\text{PP}} = 83$, 22, [P(OEt)₂], P2), 128.0 (dd, $J_{\text{PP}} = 91$, 22, [P(O)(OEt)], P3). ¹³C{¹H} NMR (100.63 MHz, C₆D₆, assignment of PC couplings from selectively decoupled spectra): δ 219.4 (dd, $J_{\text{CP3}} = 47$, $J_{\text{CP1}} = 22$, CO), 217.4 (dd, $J_{\text{CP2}} = 41$, $J_{\text{CP1}} = 22$, CO), 84.6, 84. (2 \times s, Cp), 62.8 (d, $J_{\text{CP2}} = 9$, CH₂), 62.4 (d, $J_{\text{CP1}} = 10$, CH₂), 61.5 (d, $J_{\text{CP1}} = 10$, CH₂), 61.4 (d, $J_{\text{CP2}} = 11$, CH₂), 58.1 (d, $J_{\text{CP3}} = 10$, CH₂), 17.4 (d, $J_{\text{CP3}} = 6$, Me), 16.5 (d, $J_{\text{CP1}} = 7$, Me), 16.4 (d, $J_{\text{CP2}} = 7$, Me), 16.2 (d, $J_{\text{CP2}} = 7$, Me), 16.1 (d, $J_{\text{CP1}} = 8$, Me). FAB-MS: m/z (%) 648(15) [M⁺], 621(25) [M⁺ + H – CO], 603(100) [M⁺ – OEt], 528(75) [M⁺ – CO – P(O)(OEt)]. Data for **2c** are as follows. ¹H NMR (200.13 MHz, C₆D₆): δ 4.64, 4.54 (2 \times s, 2 \times 5H, Cp), 4.70–3.70 (m, 10H, CH₂), 1.30, 1.25, 1.20, 1.19, 1.15 (5 \times t, $J_{\text{HH}} = 7$, 5 \times 3H, Me). ³¹P{¹H} NMR (80.01 MHz, C₆D₆): δ 344.9 (dd, $J_{\text{PP}} = 86$, 74, μ -P), 155.8 (dd, $J_{\text{PP}} = 74$, 9, [P(OEt)₂]), 127.7 (dd, $J_{\text{PP}} = 86$, 9, [P(O)(OEt)]).

Preparation of [Fe₂Cp₂{ μ -(EtO)₂POP(O)(OEt)}- μ -P(OEt)₂(μ -CO)] (3). A petroleum ether solution (10 mL) of compound **2a** (0.094 g, 0.26 mmol) was stirred at room temperature in a Schlenk flask without previous exclusion of air for about 3 weeks, at which point a brown suspension was formed. The solvent was then removed under vacuum, the residue was extracted with toluene, and the extract was filtered. The filtrate was concentrated under vacuum, layered with 5 mL of petroleum ether, and then allowed to mix by slow diffusion to yield black-brown crystals of compound **3** (0.028 g, 30%). Anal. Calcd for C₂₁H₃₅O₈P₃Fe₂: C, 40.67; H, 5.69. Found: C, 40.62; H, 5.67. ¹H NMR (C₆D₆): δ 5.40–5.30 (m, 2H, CH₂), 4.65, 4.40 (2 \times s, 2 \times 5H, Cp), 4.30–4.20 (m, 2H, CH₂), 4.20–4.00 (m, 2H, CH₂), 4.00–3.80 (m, 4H, CH₂), 1.48, 1.30, 1.20, 1.10, 1.02 (5 \times t, $J_{\text{HH}} = 7$, 5 \times 3H, Me). ³¹P{¹H} NMR (C₆D₆): δ 360.4 (t, $J_{\text{PP}} = 92$, μ -P), 163.2 (dd, $J_{\text{PP}} = 92$, 74, [P(OEt)₂]), 133.0 (dd, $J_{\text{PP}} = 92$, 74, [P(O)(OEt)]).

Preparation of [Fe₂Cp₂(μ -CO)₂CO](κ^1 -tedip)] (4). A cold (0 °C) toluene solution (10 mL) of tedip (0.15 mL, 0.545 mmol) was transferred over 0.100 g of [Fe₂Cp₂(CO)₃(NCMe)] (0.273 mmol) placed in a refrigerated flask at 0 °C, and the mixture was stirred at this temperature for 15 min to yield a red-violet solution. Solvent was then removed under vacuum, and the residue was dissolved in CH₂Cl₂/petroleum ether (1:2) and chromatographed at –15 °C on an alumina column (activity 3.5, 12 \times 1.5 cm) prepared in petroleum ether. Elution with the same solvent mixture gave a red fraction, containing [Fe₂-Cp₂(CO)₄], and two violet fractions. These two fractions contained compound **4** and small amounts of compound **5**, respectively. Removal of solvents from the major violet fraction yielded compound **4** (0.092 g, 58%) as a violet air-sensitive powder. ¹H NMR (CD₂Cl₂): **cis-4**, δ 4.69, 4.55 (2 \times s, 2 \times 5H, Cp), 4.00 (q, $J_{\text{HP}} = J_{\text{HH}} = 7$, 4H, CH₂), 3.94, 3.74 (2 \times m, 2 \times 2H, CH₂), 1.29 (t, $J_{\text{HH}} = 7$, 6H, Me), 1.11 (br, 6H, Me). ³¹P{¹H} NMR (CD₂Cl₂): **cis-4**, δ 165.5 (d, $J_{\text{PP}} = 12$, P–Fe), 126.4 (d, $J_{\text{PP}} = 12$, P); **trans-4**, δ 168.6 (br, P–Fe), 126.5 (br, P); **cis**: **trans** = 9:1. ¹³C{¹H} NMR (CD₂Cl₂): **cis-4**, δ 280.0 (d, $J_{\text{CP}} = 24$, 2 \times μ -CO), 215.8 (s, CO), 87.4, 86.8 (2 \times s, Cp), 61.1 (d, $J_{\text{CP}} = 6$, CH₂), 58.9 (d, $J_{\text{CP}} = 10$, CH₂), 17.0 (d, $J_{\text{CP}} = 4$, Me), 16.0 (br, Me).

(28) Perrin, D. D.; Armarego, W. L. F. *Purification of Laboratory Chemicals*; Pergamon Press: Oxford, U.K., 1988.

Preparation of $[\{\text{Fe}_2\text{Cp}_2(\mu\text{-CO})_2(\text{CO})\}_2(\mu\text{-tedip})]$ (5). The procedure is identical with that described for **4**, except that 35 μL of tedip (0.136 mmol) was used. Two violet fractions were collected, containing compounds **4** (minor) and **5** (major), respectively. Workup of the major fraction yielded compound **5** (0.100 g, 75%) as a violet powder. Anal. Calcd for $\text{C}_{34}\text{H}_{40}\text{O}_{11}\text{P}_2\text{Fe}_4$: C, 44.88; H, 4.43. Found: C, 44.80; H, 4.49. ^1H NMR (toluene- d_6): *cis,cis-5*, δ 4.49, 4.28 ($2 \times s$, $2 \times 5\text{H}$, Cp), 4.20–4.00 (m, 8H, CH_2), 1.13 (t, $J_{\text{HH}} = 7$, 12H, Me). ^1H NMR (toluene- d_6 , 253 K): *cis,cis-5*, δ 4.45, 4.34 ($2 \times s$, $2 \times 10\text{H}$, Cp), 4.06–3.90 (m, 8H, CH_2), 1.13 (t, $J_{\text{HH}} = 7$, 12H, Me); *trans,cis-5*, δ 4.55, 4.50, 4.45 ($3 \times s$, $3 \times 5\text{H}$, Cp), other resonances for this isomer obscured by those of the major isomer. *cis,cis:trans,cis* = 6:1. $^{31}\text{P}\{^1\text{H}\}$ NMR (toluene- d_6): *cis,cis-5*, δ 158.9 (s); *trans,cis-5*, δ 162.0 (br). $^{31}\text{P}\{^1\text{H}\}$ NMR (toluene- d_6 , 253 K): *cis,cis-5*, δ 159.5 (s); *trans,cis-5*, δ 163.0 (d, $J_{\text{PP}} = 80$, P), 159.4 (d, $J_{\text{PP}} = 80$, P). $^{13}\text{C}\{^1\text{H}\}$ NMR (50.33 MHz, CD_2Cl_2): *cis,cis-5*, δ 280.4 (false t, $J_{\text{CP}} + J_{\text{CP}'} = 11$, $\mu\text{-CO}$), 215.7 (s, CO), 87.6, 87.0 ($2 \times s$, Cp), 62.1 (s, CH_2), 16.0 (s, Me).

Preparation of *cis*- and *trans*- $[\text{Fe}_2\text{Cp}_2\{\mu\text{-OP}(\text{OEt})_2\}\{\mu\text{-P}(\text{OEt})_2\}(\text{CO})_2]$ (6). A toluene solution (20 mL) of compound **1** (0.300 g, 0.84 mmol) and tedip (0.26 mL, 1.06 mmol) was placed in a jacketed Pyrex flask and photolyzed at -25°C for 1 h with a N_2 purge to give a green solution. This solution was chromatographed at -15°C on an alumina column (activity 3, 30×2.5 cm) prepared in petroleum ether. Elution with CH_2Cl_2 /petroleum ether (1:1) gave a yellow fraction containing a small amount of an uncharacterized compound (IR: 2013 (w), 1961 (w), and 1923 (vs) cm^{-1} in toluene), followed by a small amount of the starting compound **1**. Elution with CH_2Cl_2 /petroleum ether (2:1) gave a green fraction containing compound *trans-6*. Finally, elution with CH_2Cl_2 /petroleum ether (3:1) gave another green fraction containing compound *cis-6*. Removal of solvents under vacuum from the last two fractions gave compounds *trans-6* (0.100 g, 23%) and *cis-6* (0.094 g, 22%) as green solids, respectively. Data for *trans-6* are as follows. Anal. Calcd for $\text{C}_{20}\text{H}_{30}\text{O}_7\text{P}_2\text{Fe}_2$: C, 43.20; H, 5.44. Found: C, 43.29; H, 5.45. ^1H NMR (200.13 MHz, C_6D_6): δ 4.51, 4.50 ($2 \times s$, $2 \times 5\text{H}$, Cp), 4.10–3.90 (m, 5H, CH_2), 3.76–3.62 (m, 3H, CH_2), 1.30, 1.29, 1.25, 1.18 ($4 \times t$, $J_{\text{HH}} = 7$, $4 \times 3\text{H}$, Me). $^{31}\text{P}\{^1\text{H}\}$ NMR (80.01 MHz, C_6D_6): δ 346.1 (d, $J_{\text{PP}} = 74$, $\mu\text{-P}(\text{OEt})_2$), 184.7 (d, $J_{\text{PP}} = 74$, $\mu\text{-OP}(\text{OEt})_2$). $^{13}\text{C}\{^1\text{H}\}$ NMR (50.33 MHz, C_6D_6): δ 222.3 (d, $J_{\text{CP}} = 29$, CO), 216.6 (dd, $J_{\text{CP}} = 42$, 24, CO), 83.5, 82.8 ($2 \times s$, Cp), 62.9 (d, $J_{\text{CP}} = 11$, CH_2), 62.4 (d, $J_{\text{CP}} = 13$, CH_2), 59.8 (d, $J_{\text{CP}} = 5$, CH_2), 57.9 (d, $J_{\text{CP}} = 10$, CH_2), 16.8 (d, $J_{\text{CP}} = 6$, Me), 16.6 (d, $J_{\text{CP}} = 7$, $2 \times \text{Me}$), 16.5 (d, $J_{\text{CP}} = 5$, Me). Data for *cis-6* are as follows. ^1H NMR (C_6D_6): δ 4.45, 4.35 ($2 \times s$, $2 \times 5\text{H}$, Cp), 4.10–3.65 (m, 8H, CH_2), 1.41, 1.22, 1.14, 1.13 ($4 \times t$, $J_{\text{HH}} = 7$, $4 \times 3\text{H}$, Me). $^{31}\text{P}\{^1\text{H}\}$ NMR (C_6D_6): δ 353.8 (d, $J_{\text{PP}} = 81$, $\mu\text{-P}(\text{OEt})_2$), 190.4 (d, $J_{\text{PP}} = 81$, $\mu\text{-OP}(\text{OEt})_2$).

Preparation of $[\text{Fe}_2\text{Cp}_2(\mu\text{-CO})_2(\mu\text{-tedip})]$ (7). A mixture of isomers **6** was prepared as described above, but starting from $[\text{Fe}_2\text{Cp}_2(\text{CO})_4]$ (0.198 g, 0.56 mmol). The crude reaction mixture was filtered and the solvent removed under vacuum. The residue was then dissolved in xylenes (12 mL) and the solution refluxed for 3 h while gently bubbling CO through it. Solvent was afterward removed from the resulting brownish solution, and the residue was dissolved in CH_2Cl_2 /petroleum ether (1:2) and chromatographed at -15°C on an alumina column (activity 3.5, 15×2.5 cm) prepared in petroleum ether. Elution with the same solvent mixture gave a yellow fraction containing a small amount of an uncharacterized compound (IR: 1950 cm^{-1} in CH_2Cl_2). Elution with CH_2Cl_2 /petroleum ether (1:1) gave a purple fraction containing compound **7**. Finally, elution with pure THF gave a yellow-orange fraction containing the compound $[\text{FeCp}\{\text{PO}(\text{OEt})_2\}(\text{CO})_2]$. Removal of solvent under vacuum from the purple fraction gave compound **7** as a violet powder (0.035 g, 15%). The crystals used in the X-ray study were grown at -20°C from a concentrated

Table 3. Crystal Data for Compound 7

mol formula	$\text{C}_{20}\text{H}_{30}\text{Fe}_2\text{O}_7\text{P}_2$
mol wt	556.09
cryst syst	orthorhombic
space group	<i>Pbca</i>
cryst color	black-violet
cryst shape	parallelepiped
radiation (λ , Å)	Mo K α ($\lambda = 0.710\ 69$ Å)
<i>a</i> , Å	18.152(8)
<i>b</i> , Å	16.066(7)
<i>c</i> , Å	16.359(8)
<i>V</i> , Å ³	4771(6)
<i>Z</i>	8
calcd density, g cm^{-3}	1.55
μ (Mo K α), cm^{-1}	13.8
diffractometer	Philips-PW 1100
temp, K	293
scan type	$\omega/2\theta$
θ limits, deg	1–25
scan width	$1.2 + 0.345 \tan \theta$
total no. of unique data	4203
no. of unique data used	1437 ($(F_o)^2 > 3\sigma(F_o)^2$)
<i>R</i> ^a	0.049
<i>R</i> _w ^b	0.052
abs coeff cor (min, max)	0.88, 1.25
no. of variables	282
$\Delta\rho_{\text{min}}$ (e Å^{-3})	–0.37
$\Delta\rho_{\text{max}}$ (e Å^{-3})	0.39

$$^a R = \sum |F_o - |F_c|| / \sum F_o. \quad ^b R_w = [\sum w(F_o - |F_c|)^2 / \sum wF_o^2]^{1/2}.$$

solution of the complex in petroleum ether. Anal. Calcd for $\text{C}_{20}\text{H}_{30}\text{O}_7\text{P}_2\text{Fe}_2$: C, 43.20; H, 5.44. Found: C, 43.51; H, 5.32. ^1H NMR (C_6D_6): δ 4.54 (s, 10H, Cp), 4.21–4.12 (m, 4H, CH_2), 4.12–4.00 (m, 4H, CH_2), 1.09 (t, $J_{\text{HH}} = 7$, 12H, Me). $^{31}\text{P}\{^1\text{H}\}$ NMR (C_6D_6): δ 179.1 (s).

X-ray Structure Determination for Compound 7. A selected crystal was set up on an automatic diffractometer. Unit cell dimensions with estimated standard deviations were obtained from least-squares refinements of the setting angles of 25 well-centered reflections. Two standard reflections were monitored periodically; they showed no change during data collection. Crystallographic data and other information are summarized in Table 3. Corrections were made for Lorentz and polarization effects. Empirical absorption correction (Difabs)²⁹ and extinction correction were applied.

Computations were performed by using the PC version of CRYSTALS.³⁰ Atomic form factors for neutral Fe, P, O, C, and H were taken from ref 31. Real and imaginary parts of anomalous dispersion were taken into account. The structure was solved by direct methods (SHELXS)³² and successive Fourier maps. Hydrogen atoms were geometrically located, and they were given an overall isotropic thermal parameter, while non-hydrogen atoms were anisotropically refined.

Full-matrix least-squares refinements were carried out in three blocks by minimizing the function $\sum w(F_o - |F_c|)^2$ where F_o and F_c are the observed and calculated structure factors, respectively. Models reached convergence with *R* and *R*_w having values defined and listed in Table 3. The weighting scheme was unity. Figure 1 represents a CAMERON³³ view of compound **7**.

Acknowledgment. We thank the Ministerio de Ciencia y Tecnología of Spain for financial support

(29) Walker, N.; Stuart, D. *Acta Crystallogr., Sect. A* **1983**, *39*, 158.

(30) Watkin, D. J.; Carruthers, J. R.; Betteridge, P. W. CRYSTALS, An Advanced Crystallographic Computer Program; Chemical Crystallography Laboratory, Oxford, U.K., 1988.

(31) *International Tables for X-ray Crystallography*; Kynoch Press: Birmingham, U.K., 1974; Vol. IV.

(32) Sheldrick, G. M. SHELXS 86, Program for Crystal Structure Solution; University of Göttingen, Göttingen, Germany, 1986.

(33) Pearce, L. J.; Watkin, D. J. CAMERON; Chemical Crystallography Laboratory, Oxford, U.K., 1989.

(Projects BQU2000-0220 and BQU2000-0944) and the Universidad de Oviedo for a grant to C.M.A.

Supporting Information Available: Tables of atomic coordinates for non-hydrogen atoms and for hydrogen atoms,

anisotropic thermal parameters, and bond lengths and angles for compound **7**. This material is available free of charge via the Internet at <http://pubs.acs.org>.

OM030201M